Cell Tissue Bank (2021) 22:305–321
https://doi.org/10.1007/s10561-020-09879-4

XRD and ATR-FTIR techniques for integrity assessment of gamma radiation sterilized cortical bone pretreated by antioxidants

Naglaa S. El-Hansi · Hoda H. Said · Omar S. Desouky · Mahmoud A. Khalaf · Mona S. Talaat · Abdelsattar M. Sallam

Received: 16 August 2020 / Accepted: 30 October 2020 / Published online: 9 November 2020

Abstract Terminal sterilization of bone allograft by gamma radiation is required to reduce the risk of infection. Free radical scavengers could be utilized to minimize the deteriorating effects of gamma radiation on bone allograft mechanical properties. The objective of this research is to assess the changes in structural and chemical composition induced by hydroxytyrosol (HT) and alpha lipoic acid (ALA) free radical scavengers in gamma sterilized cortical bone. Bovine femurs specimens were soaked in different concentrations of HT and ALA for 7 and 3 days respectively before irradiation with 35 KGy gamma radiation. The attenuated total reflection-Fourier transform infrared spectroscopy and the X-ray diffraction techniques were utilized to analyze the changes in chemical composition induced by irradiation in the presence of free radical scavengers. A significant increase in the proportion of amide I and amide II to phosphate was noticed in the irradiated group, while in the pretreated groups with ALA and HT this effect was minimized. In addition, gamma radiation reduced the mature to immature cross links while ALA and HT alleviated this reduction. No significant changes were noticed in the mineral crystallinity or crystal size. Bone chemical structure has been changed due to gamma irradiation and these changes are mainly relevant to amide I, amide II proportions and collagen crosslinks. The deteriorating effects of gamma sterilization dose (35 kGy) on chemical structure of bone allograft can be alleviated by using (HT) and (ALA) free radical scavengers before irradiation.

Keywords Bone allograft · Gamma sterilization · XRD · FTIR · Hydroxytyrosol · Alpha lipoic acid

N. S. El-Hansi (✉) · H. H. Said · O. S. Desouky
Biophysics Lab, Radiation Physics Department, Atomic Energy Authority (AEA), Nasr city, Cairo, NCRRT, Egypt
e-mail: naglaa911@yahoo.com; naglaa.elhansi@eaea.org.eg

M. A. Khalaf
Microbiology Department, (NCRRT), Atomic Energy Authority (AEA), Nasr city, Cairo, Egypt

M. S. Talaat · A. M. Sallam
Biophysics Group, Physics Department, Faculty of Science, Ain Shams University, Cairo, Egypt

Introduction

Bone allograft is used to fill a bone cavity, to enhance primary union or arthrodesis, reconstructive surgery, tumor surgery and osteoarticular reconstruction (Minamisawa et al. 1995). The risk of transmission of infectious diseases with tissue allografts is a main issue in the field of tissue banking (Kaminski et al. 2010). Microbial contamination can still exist after aseptic tissue procurement and processing techniques, so terminal sterilization of tissue allograft is necessary (Kairiyama et al. 2009).

Gamma radiation sterilization is utilized by many tissue banks (Allaveisi et al. 2015) due to its good penetrability inside matter; it enables the sterilization of materials in closed wrappings which avoid recontamination during packing and its high efficiency in the inactivation of pathogens (micro-organisms) (Bargh et al. 2020; Dziedzic-Goclawska et al. 2005). Although a radiation dose of 25 kGy is the reference dose recommended by the International Atomic Energy Agency for the sterilization of tissue grafts (Singh et al. 2016), greater doses are required to sterilize against radiation-resistant viruses (Barth et al. 2011). Gamma radiation sterilization weakens the bone mechanical properties which is a main clinical concern because bone grafts are utilized in load bearing applications (Akkus et al. 2005). The use of free radical scavengers is one of the developing strategies to overcome the detrimental effect of gamma radiation without deteriorating the sterility of bone graft (seema et al. 2008).

El-Hansi et al. 2020 found that the mechanical properties of cortical bone preatreated with HT and ALA before gamma sterilization can be preserved with maintaining the sterility assurance level. Attia et al. (2017) showed that the mechanical properties of irradiation-sterilized cortical bone allografts could be preserved by incubating the bone in a ribose solution before irradiation. Furthermore, Allaveisi et al. 2015 found that N-Acetyl-L-Cystein free radical scavenger can preserve the cortical bone against the damaging effects of ionizing radiation and could be utilized to enhance the material properties of sterilized allografts. According to a study by Willett et al. (2015), it has been found that irradiation-sterilized bone with enhanced mechanical properties can be obtained by pre-irradiation ribose treatment that led to a more stable and connected collagen network. Akkus et al. (2005) study indicated that blocking the activity of free radicals with a thiourea scavenger decreases collagen damage and helps to preserve the mechanical strength of sterilized tissue.

However, these experiments examined only the macroscopic behaviour of bone, making it difficult to establish definite predictions about how the individual phases (collagen and hydroxyapatite) are influenced by radiation in the presence of radioprotectors.

Among the techniques to assess the bone quality, Attenuated total reflection-Fourier transform infrared spectroscopy (ATR-FTIR) and X-ray diffraction (XRD) are the two major applied techniques (Sasso et al. 2018; Querido et al. 2018; Rana M et al. 2017). ATR-FTIR spectroscopy is commonly used in bone characterization studies (Paredes et al. 2017) because it provides useful information on the chemical composition and structure of both the organic and mineral phases (Sasso et al. 2018). The periodic arrangement of atoms in mineral crystals and the periodicity of the gap-overlap region of collagen fibers provide the efficacious use of X-ray diffraction (XRD) of bone nanostructure studies (Almer and Stock 2007).

The purpose of the present research is to assess the radiporotective effect of alpha lipoic acid (ALA) and Hydroxytyrosol (HT) free radical scavengers on the physicochemical properties of bovine cortical bone allograft during gamma radiation sterilization at microstructure level. XRD and ATR-FTIR techniques were used to analyze the changes in crystallinity and chemical composition induced by irradiation in the presence of free radical scavengers.

Materials and methods

Specimen preparation

Fresh bovine femurs (aged between 18–24 months) were acquired and kept frozen at − 20 C until sectioning. Before cutting, bones were first cleaned as previously mentioned by El-Hansi et al. 2020. The specimens had a thickness of 3 mm, a width of 10 mm, and a length of 70 mm. All specimens were taken from locations longitudinal to the bone long axis (Fig. 1). Four groups (10 specimens for each group) were assigned to each antioxidant: control, antioxidant

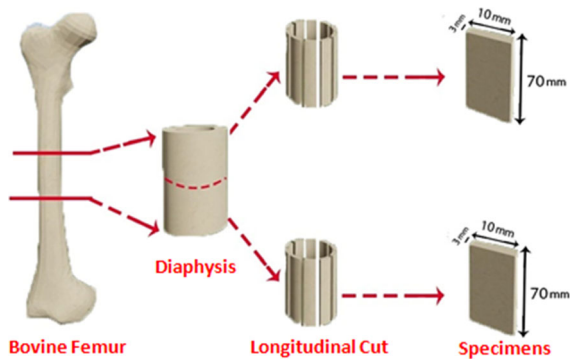

Fig. 1 The preparation processes of Bovine bone specimens

treated, irradiated and antioxidant pretreated irradiated.

Antioxidants treatment

The effect of HT and ALA on bone mechanical properties was examined through a pilot study as mentioned in El-Hansi et al. (2020).The concentrations of 9 mM ALA for 3 days and 0.25 mM HT for 7 days bone soaking, have been chosen based on this pilot study.

Gamma irradiation

Gamma cell unit (Cobalt-60, 1.85 KGy/hr) in the National Center for Radiation Research and Technology (NCRRT, Cairo, Egypt) were used for irradiation. Three groups were irradiated, two of them were first treated with HT (0.25 mM for 7 days) or ALA (9 mM for 3 days) then irradiated to 35 KGy in the presence of the antioxidant while, the other group was only irradiated to the same dose. Specimens were frozen before irradiation to reduce water mobility and subsequently free radicals production.

ATR-FTIR analysis

The infrared spectra were acquired in a Fourier transform infrared spectrometer using the platinum ATR diamond mounted on FT-IR (Bruker Vertex 70). Post irradiation, all samples were assessed in the middle infrared frequency range (from 4.000 cm^{-1} to 400 cm^{-1}) which is the appropriate range to characterize all bands from organic and inorganic compounds found in non-irradiated and irradiated samples (Zezell et al. 2015). All measurements were carried out in 4 cm^{-1} step.

ATR-FTIR evaluates the changes which occur in a totally internally reflected infrared beam as the beam comes into contact with a sample. ATR-FTIR has advantages over FTIR in that it is a rapid, non-destructive technique, spectra differences because of sample preparation is reduced (Surovell and Stiner 2001).

Related to inorganic matrix, the considered absorption bands for this study in the bone ATR-FTIR spectrum were the superposition of the $\nu_1$and $\nu_3$vibration modes of phosphate (1300–900 cm^{-1}), the $\nu_4$vibration mode of phosphate (770–480 cm^{-1}) and the ν_2 vibration mode of carbonate (890–850 cm^{-1}). The main organic absorption bands were amide I (1680–1600 cm^{-1}), amide II (1580–1480 cm^{-1}) and amide III (1300–1200 cm^{1}). The areas under the bands were calculated and the normalization of the sperctra was performed for all aforementioned absorption bands.

X-ray diffraction (XRD) analysis

Crystal structure measurements were carried out by X-ray diffractometer (Shimadzu XRD-6000) at 40 kV and 30 mA by using Cu- Kα radiation (λ = 1.5405 Å). The above mentioned operation conditions were maintained during all the relevant measurements. Each sample was scanned at 2θ scan range from 4° to 90°. The crystallite size was determined using Winfit software (Winfit 1.2-S. Krumm, Institüt für Geologie-Erlangen). Peak width at half maximum (FWHM) and peak centerline location for (002) diffraction peak were calculated over the range 25°–26.5° 2θ (Fig. 2).

Statistical analysis

The data in the current study are presented as mean ± standard deviation.SAS software (version 9) was used in performing the statistical analysis and the one way analysis of variance (ANOVA) was used in determining the significance differences between groups.

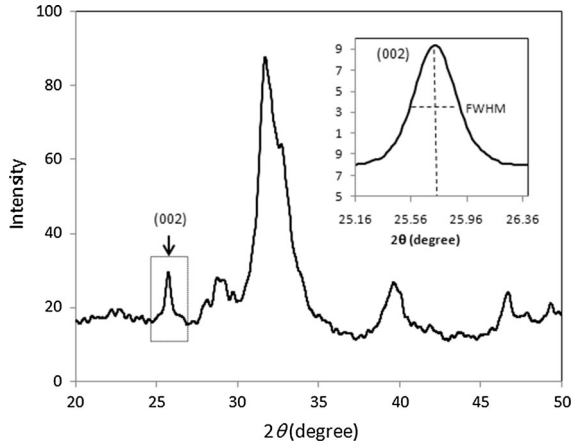

Fig. 2 XRD pattern of bovine cortical bone and (002) diffraction peak at 25.8°, which was used to determine the average crystal size in the c-direction

Results

Amide I (1680–1600 cm-1), II (1580–1480 cm-1), and III (1300–1200 cm-1) contents are relevant to the content of collagen in the hard tissue organic matrix, so the analysis of these bands may provide useful information on the conformation and denaturation of this molecule. The infrared bands of carbonate (890–850 cm^{-1}) and phosphate (1300–900 cm^{-1} and 770–480 cm^{-1}) are relevant to the carbonated hydroxyapatite, the main component of hard tissues (Figs. 3, 4).

In addition, amides to phosphate (1300–900 cm^{-1}) band areas ratios are relevant to the proportion of collagen and the hydroxyapatite, while carbonate to phosphate (1300–900 cm^{-1}) band area ratio represents the carbonate substitution level in the hydroxyapatite crystal (Fig. 5).

Each peak in the ATR-FTIR spectrum was first linearly baseline corrected between the two wavenumbers given above. The area under a band is directly proportional to the concentration of the chemical species which gives rise to the particular band. Nevertheless, it is better to use ratios between reference peak heights or areas, because the comparison parameters resulting from single band is subjected to uncertainty due to sample variations. Thus, for a semi-quantitative comparison between groups, the background signal was subtracted. After normalization by $\nu_1$and $\nu_3$vibration modes of phosphate band area (1300–900 cm^{-1}), the considered bands areas were determined. The second derivative analysis was conducted to assess the presence and position of infrared bands.

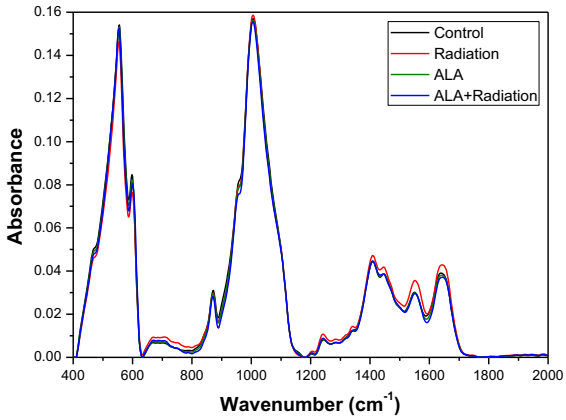

Fig. 3 ATR-FTIR spectrum of cortical bone specimens of different Alpha lipoic acid (ALA) treated groups

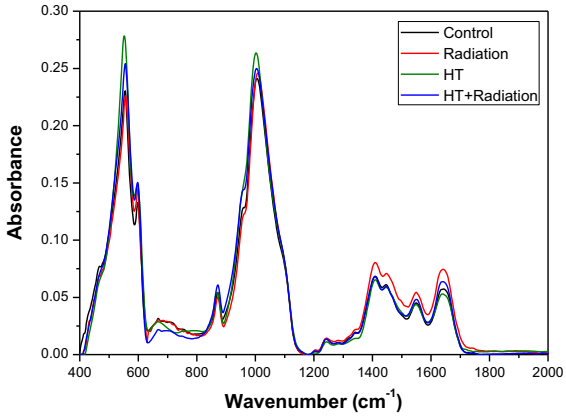

Fig. 4 ATR-FTIR spectrum of cortical bone specimens of different Hydroxytyrosol (HT) treated groups

Figures 3, 4 showed the ATR-FTIR spectra from 400–1800 cm^{-1} (fingerprint region) for different ALA and HT treatment groups respectively, which provides information of vibration modes relevant to organic and inorganic bone content. It is noted that there is no significant change in the band's detection or in the positions of the band when comparing the spectra of each group.

Figure 5a, b showed the proportion of organic (amide I, amide II and amide III) relevant to phosphate and Fig. 5b, d showed the proportion of carbonate relevant to phosphate content of the irradiated groups in the presence and absence of ALA and HT respectively. In ALA experiment, it is observed a statistically very highly significant increase (13.23%, $P < 0.001$) in the proportion of amide I to phosphate and also highly significant increase (23.81%, $P < 0.01$) in amide II to phosphate of the only irradiated group. There were not any significant changes in ALA treated group and pre-treated irradiated. In HT experiment, there was a highly significant increase (14.52%, $P < 0.01$) in the proportion of amide I to phosphate and also highly significant increase (28.57%, $P < 0.01$) in amide II to phosphate of the only irradiated group. While the pre-treated irradiated group by the specific concentration of HT showed a significantly increase in the proportion of amide I to phosphate (4.84%, $P < 0.05$) (Fig. 5a,b).

The proportion of amide II to phosphate didn't show any significant change in HT treated and

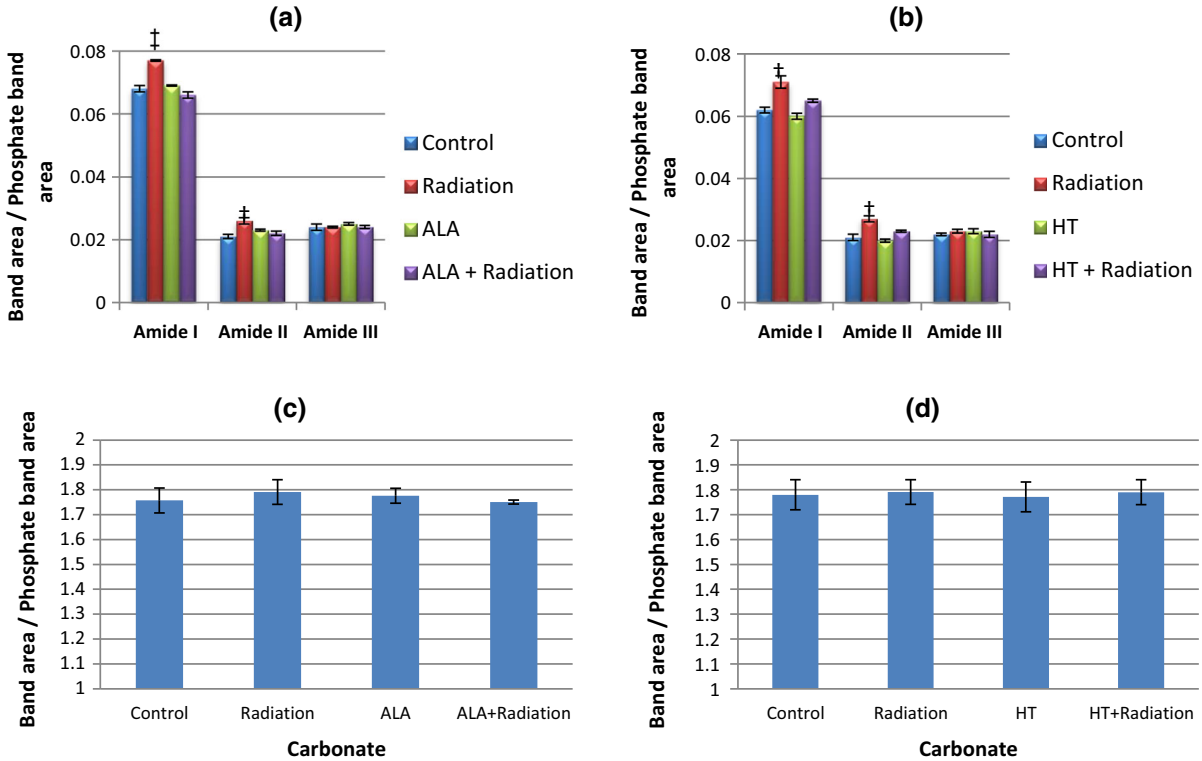

Fig. 5 a,b Means of amide I, amide II and amide III to phosphate ratios and **c,d** carbonate to phosphate ratios obtained from the cortical bone specimens of different Alpha lipoic acid (ALA) and Hydroytyrosol (HT) treatment groups. The error bars show the standard deviation of the means * $P < 0.05$, † $P < 0.01$, ‡ $P < 0.001$

pretreated irradiated groups. Also, the proportion of amide I to phosphate in HT treated group didn't show any significant change. As regards the amide III content relevant to the phosphate band, no statistical differences were observed in all groups (Fig. 5a, b). The same findings were observed when evaluating the ratio of carbonate relevant to phosphate (Fig. 5c, d).

The ATR-FTIR technique is also capable of providing quantitative information on the maturation of collagen in bones. The sub-bands of amide I bands (1660 cm^{-1} and 1690 cm^{-1}) were analyzed by conducting the second-derivative curve-fitting of the amide I peak. To deconvolute amide I band, the relevant band is separated from primary spectra of bone ranging from 1600 to 1700 cm^{-1}. And then, the second-derivative spectral analysis has been used to locate the position of the overlapping components (Figs. 6, 7). The sub-bands of amide I bands (1660 cm^{-1} and 1690 cm^{-1}), which are relevant to the collagen cross links pyridinoline (Pyr) and dihidroxinorleucine (DHLNL), were analyzed and the ratio of these bands area represent the proportion between mature and immature collagen crosslinks.

Six Gaussian peaks have been selected to fit the amide I band: 1610 cm^{-1} (aromatic rings), 1630 cm^{-1} (β-sheets), 1645 cm^{-1} (random coils), 1661 cm^{-1} (α-helix), 1678 cm^{-1} (β-sheets) and 1692 cm^{-1} (turns) (Figs. 6, 7). The above peaks were selected on the basis of the second derivative of the average spectrum of specimens and known peak-positions in the literature (Chadefaux et al. 2009).

In ALA experiment, the results indicated that gamma irradiation led to very highly significant (26.44%, $P < 0.001$) decrease in the collagen cross links ratio of the irradiated group and a significant increase (17.33%, $P < 0.05$) in ALA treated group while the pre-treated irradiated group by the specific concentration of ALA alleviated the aforementioned reduction by a noticeable percentage (23.07%) compared with the irradiated group (Table 1). In HT experiment, there was a highly significant (18.29%, $P < 0.01$) decrease in the collagen cross links ratio of

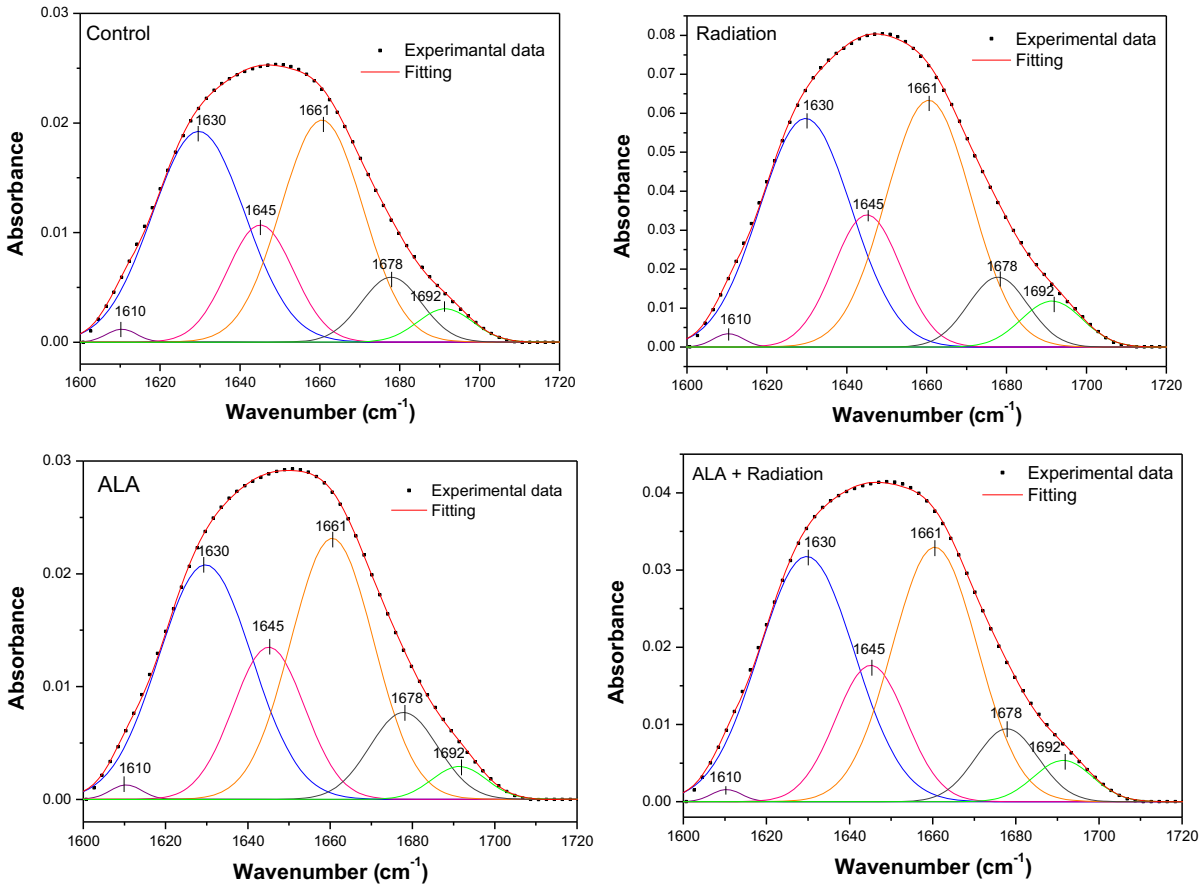

Fig. 6 Curve-fitting analysis of ATR-FTIR amide I band of cortical bone specimen in Alpha lipoic acid (ALA) group

the irradiated group and a highly significant increase (24.25%, $P < 0.01$) in HT treated group while the reduction in this ratio was alleviated by noticeable percentage (12.97%) in the HT pre-treated irradiated group when compared with the irradiated group (Table 2).

The crystallinity index (CI), which known also as splitting factor (SF), is a function of the extent of splitting of the two absorption bands at 597 $cm^{-1}$and 551 cm^{-1} correspond to A and B in Fig. 6 (Olsen et al. 2008). It provides a quantitative measure of structural order based upon the broadening of bending vibration bands of phosphate. And it is measured as described by Nagy et al. (2008). In practice, on ATR-FTIR a common baseline was made across the $\nu_4PO_3^{-4}$ band (770–480 cm^{-1}) from which the heights of points A, B and C were measured (Fig. 8).

The crystallinity index (splitting factor) was calculated according to the following equation:

$$CI = (I_A + I_B)/I_C$$

where I_{551} = intensity of 551 cm^{-1} band (A); I_{597}- = intensity of 597 cm^{-1} band (B); and I_{558} = intensity of 558 cm^{-1} band (C).

The changes in crystallinity (CI) as a result of irradiation and antioxidants treatments are shown in Fig. 9. The results revealed that the changes in mineral crystallinity in all groups are not statistically significant.

The X-ray diffraction patterns obtained from the bovine cortical bone specimens in the absence and presence of ALA and HT are shown in Figs. 10, 11 respectively. These figures presented a typical poorly crystallized pattern of hydroxyapatite in a hexagonal symmetry (Wang et al. 2010).

In order to investigate the effect of gamma radiation and radioprotecors on the crystallinity of bone allograft, the variation of the crystallite size values was calculated. As the largest dimension in bioapatite

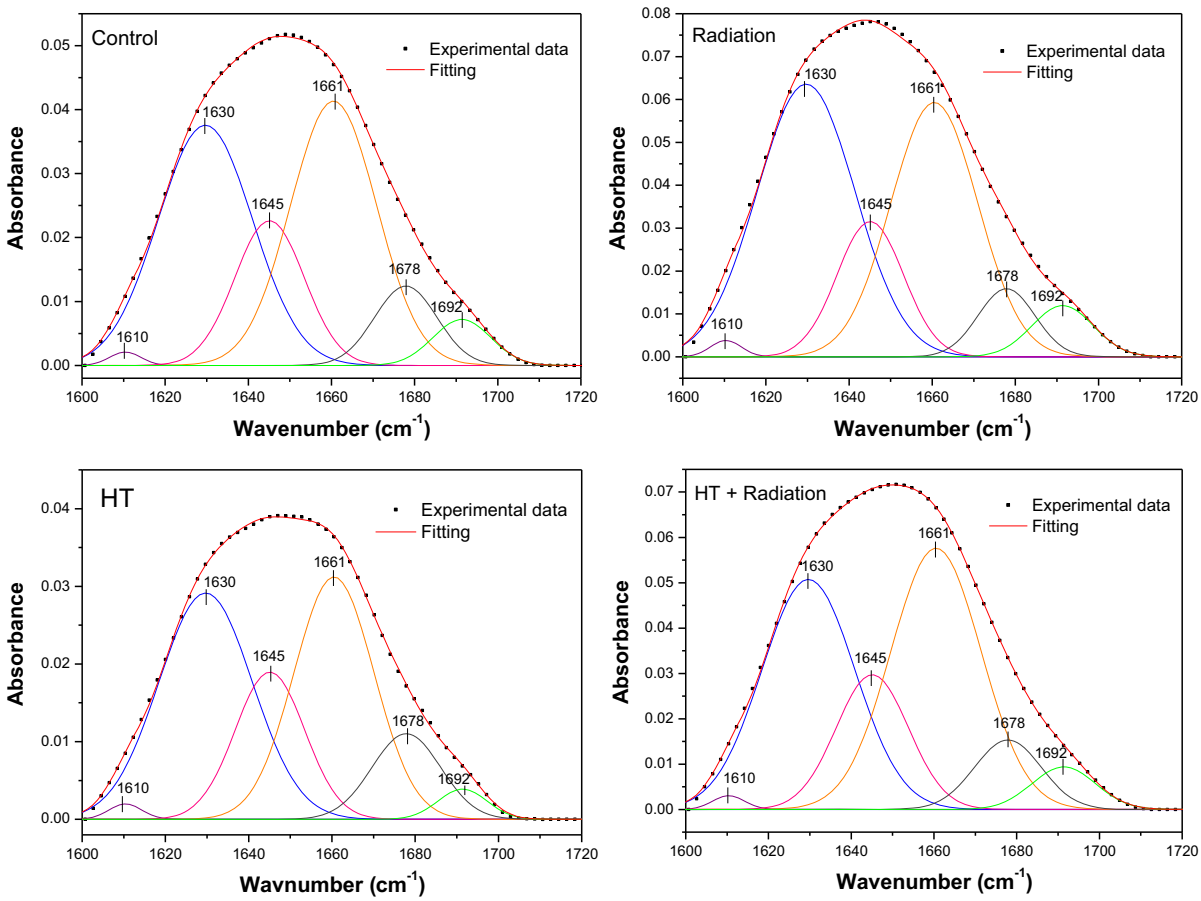

Fig. 7 Curve-fitting analysis of ATR-FTIR amide I band of cortical bone specimen in Hydroxytyrosol (HT) group

Table 1 Collagen cross linking ratio of the control and Alpha lipoic acid (ALA) treatment groups

	Collagen cross links 1660/1690
Control	9.988 ± 0.253
Radiation	7.347 ± 0.335‡
ALA	11.719 ± 0.396*
ALA + Radiation	9.042 ± 0.095*

Values indicate mean ± SD

*$P <$ 0.05, †$P <$ 0.01, ‡$P <$ 0.001

Table 2 Collagen cross linking ratio of the control and Hydroxytyrosol (HT) treatment groups

	Collagen cross links 1660/1690
Control	8.621 ± 0.322
Radiation	7.044 ± 0.243†
HT	10.712 ± 0.396†
HT + Radiation	7.958 ± 0.342

Values indicate mean ± SD

*$P <$ 0.05, †$P <$ 0.01, ‡$P <$ 0

crystals is typically parallel to the c-axis, the changes in (002) data are relevant to the lattice parameters along the crystal length. Thus, the characteristic peak at 25.8° for the (002) plane was used to measure the size of the apatite crystals (Wang et al 2010). So each 002 diffraction peak at about 25.8° (2θ) in the XRD patterns was isolated from the neighboring peaks, and therefore was able to measure the FWHM value for the 002 diffraction. Tables 3, 4 listed the obtained crystal size values for the 002 diffraction peak along the c-axis. It is worthy to note that the relative high

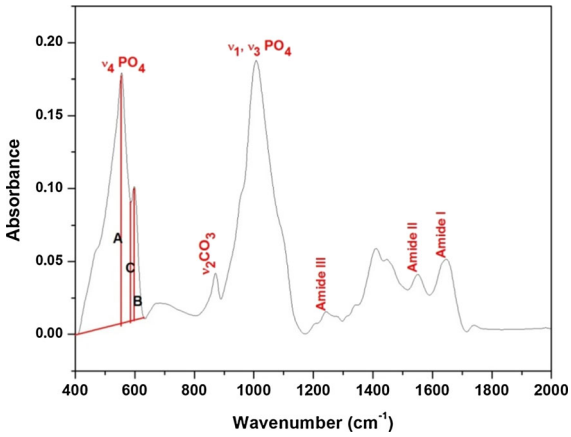

Fig. 8 The ATR-FTIR spectrum of bovine cortical bone between wavenumbers (400 and 2000 cm^{-1})

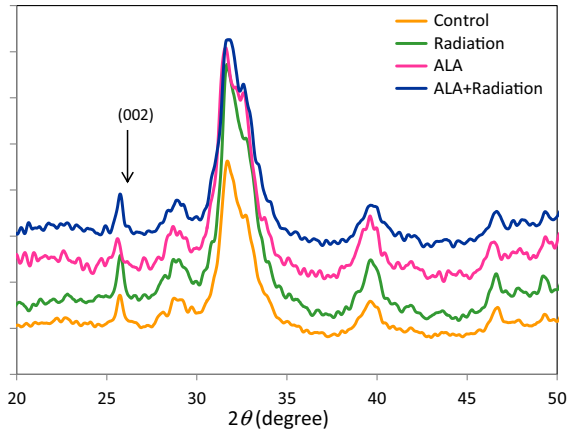

Fig. 10 XRD patterns of cortical bone specimens of different Alpha lipoic acid (ALA) treated groups

intensity of the base-line observed in XRD patterns (as clearly shown in Fig. 2) may be attributed to the presence of amorphous material and/or overlapping with the diffraction effect of collagen (Alessandro et al 2015). Statistical analysis showed that the changes in all groups are non-significant (Table 3, 4).

Discussion

Bone is a multi-phase hierarchical structure comprising of inorganic and organic components, and water (Allaveisi et al. 2013). The organic fraction is predominantly collagen with 20–30% in the entire bone tissue and 90% in the organic component (Chadefaux et al. 2009). Type I collagen represents 85–90% of the total bone protein (Barth et al. 2011). Bone also contains non-collagenous proteins, lipids and water (about 10%). The major inorganic matrix part is hydroxyapatite crystal, which has a structure similar to calcium hydroxyapatite $Ca_{10}(PO_4)_6(OH)_2$ mineral (Paschalis et al. 2017) and it represents 60–70% of the bone tissue (Chadefaux et al. 2009). The mechanical properties of bone are highly dependent on its micro-structural properties (Potdevin et al. 2012). The degree of crystallinity and ion substitution (carbonate substitution in HAP) of the hydroxyapatite (HAP) regulates bone stiffness response (Chauhan et al. 2018) while the collagen plays a major role in impacting the postyield properties and the overall

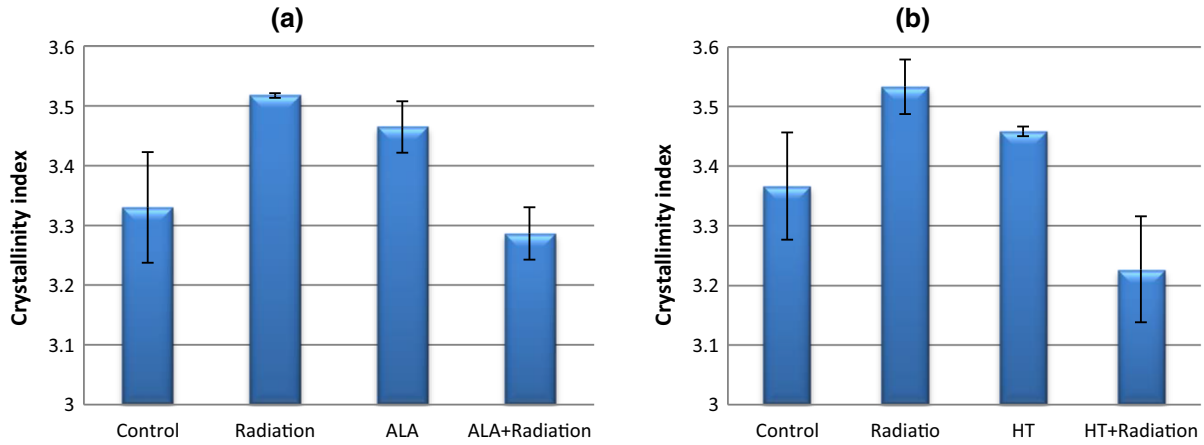

Fig. 9 **a,b** Mean values of cortical bone crystallinity index at different Lipoic acid (ALA) and Hydroxytyrosol (HT) treatment groups respectively. The error bars show the standard deviation of the means.* $P < 0.05$, † $P < 0.01$, ‡ $P < 0.001$

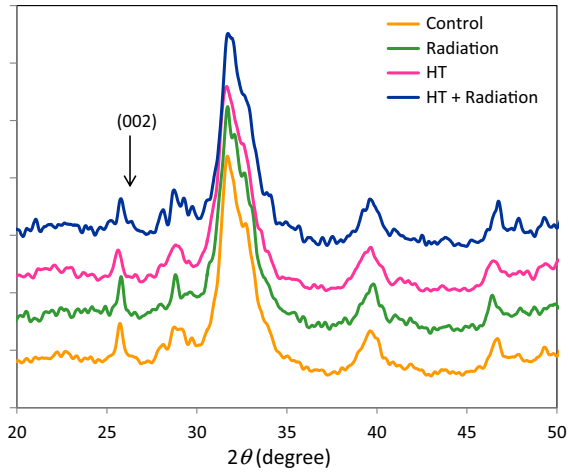

Fig. 11 XRD patterns of cortical bone specimens of different Hydroxytyrosol (HT) treated groups

Table 3 Crystal size of the control and Alpha lipoic acid (ALA) treatment groups obtained from XRD

	Crystal size (nm)
Control	18.9 ± 0.091
Radiation	18.95 ± 0.751
ALA	18.5 ± 0.319
ALA + Radiation	18.75 ± 0.29

Values indicate mean ± SD $*P < 0.05$, $\dagger P < 0.01$, $\ddagger P < 0.001$

Table 4 Crystal sizes of the control and Hydroxytyrosol (HT) treatment groups obtained from XRD

	Crystal size (nm)
Control	17.25 ± 1.328
Radiation	17.45 ± 0.405
HT	17.35 ± 0.29
HT + Radiation	17.15 ± 0.578

Values indicate mean ± SD $*P < 0.05$, $\dagger P < 0.01$, $\ddagger P < 0.001$

toughness of bone tissue (Wang et al. 2002). The deterioration of either the collagen or the mineral may have a major and unpredictable influence on the entire mechanical and material properties of the bone, making it difficult to determine the contribution of each bone (Burr 2002).

Gamma irradiation is commonly used for terminal sterilization of bone allografts. It detrimentally affects the mechanical properties of bone allografts on a dose-dependent manner (Nguyen et al. 2007). The deteriorated effects of gamma irradiated bone occur through two mechanisms: direct and indirect effects. Directly, gamma irradiation causes scission sites in the polypeptide chains (Dziedzic-Goclawska et al. 2005). Indirectly, gamma rays induce water molecule radiolysis, creating free radicals and attacking collagen rather than minerals in the bone matrix (Akkus and Belaney 2005). Collagen contains a considerable amount of water bound to its structure, which make it the main object for radiation damage and consequently loss of bone collagen connectivity and toughness (Atria et al. 2017). Cross-linking reactions have been observed during the irradiation of collagen in the presence of water (indirect effect), possibly because of the action of highly reactive, short-lived hydroxyl radicals (* OH) resulting from water radiolysis (Dziedzic-Goclawska et al. 2005).

The appropriate radioprotectant for bone allograft treatment must: be biocompatible; penetrate into the bone matrix; dissolve in water; and never protect the pathogens (Kattaya et al. 2008). Additionally, its molecular weight should be less than 300 Da because compounds beyond this molecular weight could not penetrate the bone tissue (Tami et al. 2003). ALA (206.32 Da) is a natural antioxidant synthesized by plants and animals; including humans (Self et al. 2000) also it has a high bioavailability in vivo and in vitro (Bustamante et al. 1998). Smith et al. 2004 concluded that ALA has the capacity to regenerate a variety of oxidized antioxidants to their active antioxidant forms. ALA stimulates the formation of bone tissue in ovariectomized (OVX) rats in a dose-dependent manner (Radzki et al. 2016) and it has the capacity to stimulate the healing of femoral fractures in rats (Aydin et al. 2014). In addition ALA has been shown to stimulate osteoblast formation, suppress osteoblast apoptosis and improve bone formation in vitro and inhibit bone loss in vivo (Sun et al. 2014). ALA suppresses the activity of bone-resorbing osteoclasts via its ability to scavenge reactive oxygen species (ROS) in inflammation-driven osteoclastogenesis models (Roberts and Moreau 2015).

Another natural antioxidant, Hydroxytyrosol (3,4-dihydroxyphenylethanol-154.16 Da) is one of the major phenolic components of olive oil found in the

fruit and leaves of the olive (Vilaplana-Pérez et al. 2014) and it is an efficacious scavenger of many free radicals (Martínez et al. 2018). Hagiwara et al. (2011) investigated in vitro and in vivo the effects of enormous polyphenols in olives on bone formation and maintenance. The experiments demonstrated that hydroxytyrosol induced the deposition of calcium and reduced H_2O_2 levels in dose-dependent manner. Hydroxytyrosol has also been found to suppress the formation of multinucleated osteoclasts in culture. Puel et al. (2008) showed that HT avoided a decrease in total femoral, diaphyseal and metaphyseal bone mineral density. The study of Medina-Martínez et al. (2016) showed that hydroxytyrosol has an antibacterial effect against a wide variety of bacteria. Additionally HT has been described as a special class of HIV-1 inhibitors that prevent HIV from penetrating the host cell and binding the HIV-1 catalytic site, inhibiting both viral entry and integration (Bedoya et al. 2016). Our study tested the potential of both antioxidants to enhance the chemical composition and structure of mineral and organic phase of cortical bone irradiated with gamma radiation.

Biological molecular bonds with an electric dipole moment which would be altered by atomic displacement caused by natural vibrations are infrared active and thus are quantitatively measured by infrared spectroscopy (Baker et al. 2014). Thus infrared spectroscopy could be used in characterizing biological materials and providing information on the biochemistry of the analyzed tissue (Severcan and Haris 2012). The intensity, position and width of a vibrational band obtained with an infrared spectroscopy could be used in different conditions to monitor a particular functional group or molecule (Severcan and Haris 2012). ATR-FTIR technique is used in analyzing compositional and structural changes of mineralized tissue. Also it has been utilized to assess different conditions which could alter bone structure and composition which affect its mechanical properties (Lopes et al. 2018). In this study, ATR-FTIR spectroscopy has been utilized to analyze the chemical changes in the sterilized cortical bone by calculating parameters relevant to bone quality such as amides to phosphate (matrix to mineral) ratio, collagen maturity, carbonate to phosphate ratio and mineral crystallinity.

Throughout this study, the ratio of organic components (amide I, amide II and amide III) to phosphate (1300–900 cm-1) band area was determined in order to verify changes in bone composition (Fig. 4a, b). Amide I, amide II and amide III bands analysis are relevant to bone organic content, which mainly relevant to the type-I collagen.

Amide I (1600–1700 cm^{-1}) is the most intense absorption band of collagen protein. Collagen has a three-dimensional helical structure formed by polypeptide chains, three of which coil together to create a right-handed twist triple helix structure (Cox and Nelson 2008). The intensity, position and shape of this band encode the secondary configuration of proteins that in native proteins is α-helix (Mavrogenis et al. 2016). The amide I band is regulated by the stretching vibrations of the C–N and C=O groups in collagen protein (Krimm and Bandekar 1980). Amide II and amide III bands are also relevant to the organic content of bone, and relevant to collagen secondary structure. Amide II band is the next intense absorption band at which is assigned to β-turns of the proteins (Mavrogenis et al. 2016). Both amide II and amide III are corresponding to the combination of N–H in-plane bending and C–N stretching vibrations (Vidal and Mello 2011). The distinction between amide II and III is the relative contribution of these modes to the respective mixed vibrations where the N–H bending mode makes a greater contribution to amide II, the opposite happens for amide III band (Figueiredo et al. 2012). Mavrogenis et al. (2016) found that the vibrations formed by amide I and amide II groups are very sensitive to ionizing radiation, especially amide II is more sensitive to conformational changes.

In our study, it is observed a statistically very highly significant increase (13.23%) in the proportion of amide I to phosphate and also highly significant increase (23.81%) in amide II to phosphate of the only irradiated group in ALA experiment. In HT experiment, there was a highly significant increase (14.52% and 28.57%) in the proportion of amide I and amide II to phosphate of the only irradiated group respectively in Fig. 5a, b.This indicated that gamma radiation has induced changes in helical structure of collagen. Such findings support the results of Zezell et al. 2015, who reported that the amide II significantly increased as the doses of gamma increased 0.01- 75 KGy. Also Barth et al. 2010 showed that Deep UV-Raman spectra display a very marked increase in amide I peak after x-ray exposure (70 KGy) resulting in severe collagen damage as the dose of irradiation increase.

Collagen cross-links can be divided into: enzymatic immature divalent cross-links, mature trivalent pyridinoline and pyrrole cross-links, and non-enzymatic cross-links (advanced glycation end products) (Saito et al. 2010). Buehler (2011) reported that intermolecular cross-linking provides viscoelasticity and tensile strength for the fibrillar matrices. The cross-links hold the array of type I collagen in conformity; thus collagen's capacity to absorb energy declines when cross-links increase and break apart when they decrease (Barth et al. 2011). Collagen maturity is evaluated by the 1660/1690 cm^{-1} sub-bands ratio of the amide I band where component of the amide I band at 1660 cm^{-1} has been reported to be related to enzymatic mature type I trivalent cross-link pyridinoline (Pyr) (Gamsjaeger et al. 2017), and that at 1690 cm^{-1} is related to enzymatic immature divalent cross-links dihidroxinorleucine (DHLNL) (McNerny et al. 2015).The relative percentage of the two sub-bands area ratio gives a semi-quantitative measure of the profile cross-linking in collagen matrix and is relevant to the abundance of these cross links collagen in mineralized tissue (Barth et al. 2011).

Results showed that the 1660:1690 peak areas ratio decreased by (26.44%) and (18.29%) in ALA and HT experiments respectively with 35 kGy of irradiation, revealing significant changes in the cross-linking amide I region (Tables 1and 2). Any reduction in mature cross-links or an increase in immature cross-links could disrupt the mature cross-links integrity, contributing to premature mechanical failure of the bone (Barth et al. 2011).

Results obtained in this study are in agreement with a previous study of Barth et al. (2011) who found that the non-reducible to reducible crosslinks ratio in the collagen decreased in irradiation-damaged bone at dose of 70 kGy. The deviation from the normal distribution of these cross-links lead to gradually disruption in the mature cross-links integrity, resulting in lower fracture loads. Bone toughness is mainly provided by the organic matrix, and the collection of covalent collagen cross-links is responsible for stabilizing this polymeric network (Garnero 2012; McNerny et al. 2015). Collagen crosslinks add stability to the organic matrix, avoiding microfibrils from slipping past each other (Unal et al. 2018) and affects mainly the post-yield properties of bone, as pre-yield strength is mainly dependent on the mineral phase (Garnero 2012). In the mouse model of lathyrism (lysyl oxidase inhibition by toxin), McNerny et al. (2015) found a positive correlation between the ability of the cortical bone to resist crack growth (notch produced in the femur diaphysis to determine fracture toughness) and the ratio of mature to immature enzymatic crosslinks Mata-Miranda et al. 2019 concluded that bone fractures exhibited changes in its biochemical composition, indicating bone immaturity. The cross-link ratio relevant to matrix maturity was found to be lower in the stress fracture group compared to the healthy bone.

In our study the pre-treated irradiated group by the specific concentrations of ALA and HT alleviated the reduction in collagen maturity by a noticeable percentage (23.07% and 12.97%) respectively compared with the irradiated group (Tables 1and 2). Our results showed that irradiation-sterilized bone with enhanced mechanical properties could be obtained by applying ALA and HT pre-irradiation treatment, that provides a more stable and connected collagen network than that found in irradiated controls. Blocking free radical activity with ALA and HT scavengers reduces the degree of collagen damage and helps to preserve the mechanical strength of the sterilized tissue.

Daniele et al. 2017 concluded that ALA has the capacity to recapture many free radicals such as hydroxyl radical, hypochlorous acid and peroxyl radicals. HT is an efficacious scavenger of several free radicals (Martínez et al. 2018) and is also a powerful scavenger of hydroxyl radicals (Rietjens et al. 2007). There are two probable mechanisms that could preserve the bone: (1) ALA and HT protect the bone from free radicals which originate during irradiation. Gamma irradiation induces radiolysis of water molecules and hence produces free radicals (Akkus et al. 2005; Nguyen et al. 2007) which are the main contributor to the loss of collagen connectivity and bone toughness (Akkus et al. 2005; Seto et al. 2009). Our study showed that the ALA and HT pre-treatment protect the helical structure of collagen in the irradiated samples due to their powerful capacity in recapturing many free radical species. (2) ALA and HT induced crosslinking resulting in increased stability and connectivity of the collagen network that could preserve the collagen from the chain scission during gamma sterilization. This is indicated in ALA and HT treated groups which led to significant increase (17.33%, $P < 0.05$) and highly significant increase

(24.25%, $P < 0.01$) in collagen cross links ratio (Tables 1 and 2) respectively.

Carbonate ions account for around 6–7% of the total mineral ions in bone minerals, therefore a non-negligible proportion. Carbonate ions could be incorporated into bone mineral by substitution in the apatite lattice of either PO43-(major site, type B carbonate) or OH-(minor site, type-Acarbonate) and the third site of CO_3^{2-} ion corresponds to labile carbonates that decrease with the maturation of the apatite crystal (Rey et al. 1991). In infrared spectroscopy, carbonate content is evaluated using out-of-plane bending vibration mode of the ν_2CO_3 band (around 780) and was generally calculated as CO_3/PO_4 area ratio (Farlay and Boivin 2012). Carbonate to phosphate ratio represents the degree of carbonate incorporation into the lattice of hydroxyapatite (Lopes et al. 2018) and provides information on the quality of minerals or the chemical composition of bones which changes with bone morphology, age and mineral crystallinity (Yerramshetty et al. 2006). Akkus et al. (2004) stated that in the mouse model test, the bone stiffness and bending modules were significantly dependent on the degree of mineralization, mineral crystallinity, and B-type carbonate substitution. In our study, there was not any statistical difference between CO_3/PO_4 ratios of gamma irradiated or antioxidant treated groups Fig. 5c, d. The same finding was found in the study of Zezzel et al. (2015) who used mid-infrared spectroscopy to determine the effect of ionizing irradiations (0.01–75 KGy) on hard tissue chemical structure. They did not observe any statistical difference in CO_3/PO_4 ratio.

Bone mineral is a poorly crystalline; nanocrystalline carbonated apatite with no other observable calcium phosphate phases present and includes several ion and cationic substitutions, such as HPO4, Na, and Mg (Glimcher 1998). Mineralized bone matrix properties play a critical role in assessing bone quality and fracture resistance. Donnelly et al. (2010) found that the mineral nanocrystals have major effects on bone strength. Also Boskey (2003) discussed the relationship and the significance of apatite crystallinity to bone mechanical properties. ATR spectroscopy presents powerful tool to evaluate bone mineral crystallinity. With ATR spectra, three approaches are commonly used as directly proportional to apatite crystallinity: the splitting resolution of the two ν_4PO_4 bands (asymmetric bending vibration) (Weiner and Baryosef 1990), the ratio of the peak height intensities of the 1030 and 1020 cm^{-1}subbands of the ν_3PO_4 band (asymmetric stretching vibration) (Camacho et al. 1999) and from the inverse of bandwidth at the half peak intensity of the prominent PO_4^{3-} band at 960 cm^{-1} (Freeman et al. 2001).

In this study, crystallinity was evaluated by calculating the splitting factor (SF) which is a measure of the order of the crystal structure and composition within bone (Fig. 8), the higher the SF the more crystalline the structure (Fredericks et al. 2012). The change in crystallinity of osteoporotic cortical bone led to the alteration of nanomechanics, and the increasing of crystallinity was complainant with the duration of estrogen withdrawal (The estrogen withdrawal induced by ovariectomized surgery, affected the mineral and collagen properties of cortical bone) (Wen et al. 2015) Yerramshetty and Akkus (2008). reported that tissue strength and stiffness increased with increasing crystallinity, while the ductility decreased.

In this work, the use of 35 kGy gamma irradiation and radioprotectors treatment showed no significant change in crystallinity of cortical bone hydroxyapatite (Fig. 9). Results obtained in this study are in agreement with a previous study of (Zezzel et al. 2015) where they used FTIR technique to assess the effects of various doses of gamma radiation (0.01–75 KGy) on bone tissue. They found that low doses of gamma radiation reduced bone crystallinity but the crystallinity is not altered after 0.1 kGy. Also by evaluating the effects of gamma radiation on the bone by Raman spectroscopy, Kubisz and Polomska (2007) showed that no changes in the inorganic component were observed at any dose used (from 10 kGy up to 1000 kGy) Veloso et al. (2013). also suggested that until 0.1 kGy the dose affects the hydroxyapatite crystal in order to disorganize it, however the crystal returns to be organized at highest doses values (1-75KGy).

In this study, X-ray diffraction has been used in conjunction with ATR spectroscopy to obtain the maximum amount of structural information about the effect of radioprotectors treatment on sterilized cortical bone. In X-ray diffraction pattern, the crystallite size could be represented by the diffracting plane (002) of HAP at $2\theta = 25.50°$, since this miller index corresponds to the *c*-axis length which is the direction of maximum elongation. The full width at half

maximum (FWHM) of the 002 reflection is inversely proportional to the crystallite length along the *c* unit cell direction (*c*-axis length) (Pleshko et al. 1991). Bone mineral crystal size and perfection impair the ability of bone composites to react to loads where bones with a prevalence of larger crystals than optimal will have decreased resistance to load (i.e. would be more brittle) (Boskey 2003). When Noor et al. (2011) analyzed the structure of hydroxyapatite crystals by X-ray diffraction (XRD), they found a larger crystal size in osteoporotic bone relative to normal bone, suggesting higher porosity. The materials with a higher porosity level have poorer mechanical properties, possessing greater fragility, lower hardness, and lower flexibility, in consequence of the weaker bonds between the bone crystals (Noor et al. 2011). The increased crystal size could affect the crystallinity detected by FTIR (Paschalis et al. 1996).

In this work, the XRD analysis revealed that there were not any significant change in crystal size between irradiated and antioxidant pre-treated groups (Tables 3 and 4). This is in agreement with Rana et al. 2017 who studied the effect of 25 kg gamma irradiation on the extracted HA from bovine and human bone. The XRD patterns of the HA have not shown any significant differences between the control and irradiated samples.

The chemical structure of bone tissue is highly correlated with its mechanical properties. In this way, changes in chemical structure also promote changes in mechanical properties of bone tissue (Barth et al. 2011). Wang et al. (2001) concluded that denaturation of collagen without a change in bone mineral significantly reduces the toughness and overall strength of the bone, while having minimal effects on elastic modulus. This emphasizes the positive contribution of collagen in raising the energy needed for bone failure. Another study of Zioupos et al. (1999) concluded that collagen may not contribute significantly to the strength and stiffness of the whole bone, or bone matrix. It is apparent from the respective elastic moduli of hydroxyapatite (114 GPa) and collagen (1.5 GPa). Wang and coworkers (2002) reported that collagen could be the main toughening mechanism in bone, which has a greater effects on bone toughness than on strength or stiffness (Zioupos et al. 1999). Previous studies have concluded that the macroscopic elastic properties of tissues, calculated by three-point bend tests, remain unchanged at radiation doses up to 630 kGy (Barth et al. 2010) as they are mainly influenced by the properties of the mineral phase that are less susceptible to radiation damage (Franzel and Gerlach 2009).

Data of present study demonstrated that the pre-treatment with HT and ALA before irradiation alleviated the damage of collagen, while crystallinity and crystal size were not significantly affected by gamma irradiation nor indeed the combination of antioxidants pre-treatment and irradiation.

Conclusion

The effect of gamma irradiation sterilization in the absence and presence of the HT and ALA free radical scavenger, on the physicochemical properties of bone constituents (mineral and collagen) of bovine cortical bones was studied using ATR-FTIR and XRD spectroscopy. Bone molecular structure has been changed due to gamma irradiation and these changes are mainly relevant to amide I, amide II proportions and collagen crosslinks. The deteriorating effects of gamma sterilization dose (35 kGy) on microstructure of bone allograft can be alleviated by using the proposed concentrations of HT and ALA free radical scavenger.

Acknowledgements This manuscript has been resulted from a Ph.D. research project carried out by the 1st author under the supervision of the other authors as the project supervisors at Radiation Physics and Microbiology Departments in Egyptian Atomic Energy Authority (AEA) and at Biophysics Group in Physics Department, Faculty of Science, Ain Shams University in Cairo.

Funding This research did not receive any specific grant from funding agencies in the public, commercial, or not-for-profit sectors.

Compliance with ethical standards

Conflict of interest There is no conflict of interest regarding this article.

References

Akkus O, Adar F, Schaffler MB (2004) Age-related changes in physicochemical properties of mineral crystals are related to impaired mechanical function of cortical bone. Bone 34(3):443–453. https://doi.org/10.1016/j.bone.2003.11.003

Akkus O, Belaney RM (2005) Sterilization by gamma radiation impairs the tensile fatigue life of cortical bone by two orders of magnitude. J Orthop Res 23:1054–1058. https://doi.org/10.1016/J.Orthres.2005.03.003

Akkus O, Belaney RM, Das P (2005) Free radical scavenging alleviates the biomechanical impairment of gamma radiation sterilized bone tissue. J Orthop Res 23:838–845. https://doi.org/10.1016/j.orthres.2005.01.007

Alessandro N, Paola T, Adriana B, Piermaria F, Milena F, Lorenzo M (2015) Incorporation of nanostructured hydroxyapatite and poly (N-isopropylacrylamide) in demineralized bone matrix enhances osteoblast and human mesenchymal stem cellactivity. Biointerphases 10(4):041001. https://doi.org/10.1116/1.4931882

Allaveisi F, Hashemi B, Mortazavi SM (2013) Effect of gamma sterilization on microhardness of the cortical bone tissue of bovine femur in presence of Nacetyl-L-cysteine free radical scavenger. Phys Med 30(3):314–319. https://doi.org/10.1016/j.ejmp.2013.09.004

Allaveisi F, Hashemi B, Mortazavi SM (2015) Radioprotective effect of N-acetyl-L-cysteine free radical scavenger on compressive mechanical properties of the gamma sterilized cortical bone of bovine femur. Cell Tissue Bank 16:97–108. https://doi.org/10.1007/s10561-014-9446-9

Almer JD, Stock SR (2007) Micromechanical response of mineral and collagen phases in bone. J Struct Biol 157(2):365–370. https://doi.org/10.1016/j.jsb.2006.09.001

Attia T, Woodside M, Minhas G, Lu XZ, Josey DS, Burrow T, Grynpas M, Willett TL (2017) Development of a novel method for the strengthening and toughening of irradiation-sterilized bone allografts. Cell Tissue Bank 18:323–334. https://doi.org/10.1007/s10561-017-9634-5

Aydin A, Halici Z, Akoz A, Karaman A, Ferah I, Bayir Y, Aksakal AM, Akpinar E, Selli J, Kovaci H (2014) Treatment with α-lipoic acid enhances the bone healing after femoral fracture model of rats. Naunyn-Schmiedeberg's Arch Pharmacol 387:1025–1036. https://doi.org/10.1007/s00210-014-1021-1

Baker M, Trevisan J, Bassan P et al (2014) Using Fourier transform IR spectroscopy to analyze biological materials. Nat Protoc 9(8):1771–1791. https://doi.org/10.1038/nprot.2014.110

Bargh S, Silindir-Gunay M, Ozer AY, Palaska E, Karaarslan D, Ide S, Solpan D (2020) Physicochemical evaluation of gamma and microwave irradiated dental grafts. Radiat Phys Chem 170:108627. https://doi.org/10.1016/j.radphyschem.2019.108627

Barth HD, Launey ME, Macdowell AA, Ager JW 3rd, Ritchie RO (2010) On the effect of X-ray irradiation on the deformation and fracture behavior of human cortical bone. Bone 46(6):1475–1485. https://doi.org/10.1016/j.bone.2010.02.025

Barth HD, Zimmermann EA, Schaible E, Tang SY, Alliston T, Ritchie RO (2011) Characterization of the effects of x-ray irradiation on the hierarchical structure and mechanical properties of human cortical bone. Biomaterials 32(34):8892–8904. https://doi.org/10.1016/j.biomaterials.2011.08.013

Bedoya LM, Beltrán M, Obregón-Calderón P, García-Pérez J, Torre H, González N, Pérez-Olmeda M, Auñón D, Capa L, Gómez-Acebo E, Alcamí J (2016) Hydroxytyrosol: a new class of microbicide displaying broad anti-HIV-1 activity. AIDS 30(18):2767–2776. https://doi.org/10.1097/QAD.0000000000001283

Boskey A (2003) Bone mineral crystal size. Osteoporos Int 14(5):1433–2965. https://doi.org/10.1007/s00198-003-1468-2

Buehler MJ (2011) Multiscale aspects of mechanical properties of biological materials. J Mech Behav Biomed Mater 4(2):125–127. https://doi.org/10.1016/j.jmbbm.2010.12.018

Burr DB (2002) The contribution of the organic matrix to bone's material properties. Bone 31(1):8–11. https://doi.org/10.1016/S8756-3282(02)00815-3

Bustamante J, Lodge JK, Marcocci L, Tritschler HJ, Packer L, Rihn BH (1998) α-lipoic acid in liver metabolism and disease. Free Rad Bio Med 24(6):1023–1039. https://doi.org/10.1016/S0891-5849(97)00371-7

Camacho NP, Rinnerthaler S, Paschalis EP, Mendelsohn R, Fratzl P (1999) Complementary information on bone ultrastructure from scanning small angle X-ray scattering and fourier-transform infrared microspectroscopy. Bone 25(3):287–293. https://doi.org/10.1016/S8756-3282(99)00165-9

Chadefaux C, Ho AL, Bellot-Gurlet L, Reiche I (2009) Curve-fitting micro-ATR-FTIR studies of the amide I and II bands of type I collagen in archaeological bone materials. E-Preservation Science 6:129–137. Corpus ID: 51766283

Chauhan S, Khan SA, Prasad A (2018) Irradiation-induced compositional effects on human bone after extracorporeal therapy for bone sarcoma. Calcif Tissue Int 103:175–188. https://doi.org/10.1007/s00223-018-0408-2

Cox MM, Nelson DL (2008) Lehninger Principles of Biochemistry, 5th ed. Palgrave Macmillan. ISBN: 9780230226999, 023022699X

Daniele T, Giovanni LV, Cesarina G, Sonia G, Daniele T, Carmelina DA, Gabriella L, Francesco A, Roberto A, Vincenzo B (2017) Biochemical and clinical relevance of alpha lipoic acid: antioxidant and anti-inflammatory activity, molecular pathways and therapeutic potential. Inflamm Res 66:947–959. https://doi.org/10.1007/s00011-017-1079-6

Donnelly E, Chen DX, Boskey AL, Baker SP, van der Meulen MC (2010) Contribution of mineral to bone structural behavior and tissue mechanical properties. Calcif Tissue Int 87:450–460. https://doi.org/10.1007/s00223-010-9404-x

Dziedzic-Goclawska A, Kaminski A, Uhrynowska-Tyszkiewicz I, Stachowicz W (2005) Irradiation as a safety procedure in tissue banking. Cell Tissue Bank 6:201–219. https://doi.org/10.1007/s10561-005-0338-x

El- Hansi NS, Sallam AM, Talaat MS, Said HH, Khalaf MA, Desouky OS (2020) Biomechanical properties enhancement of gamma radiation sterilized cortical bone using antioxidants. Radiat Environ Biophys 59(3):571–581. https://doi.org/10.1007/s00411-020-00848-9

Farlay D, Boivin G (2012) Bone mineral quality. In: Dionyssiotis Y (eds) Osteoprosis, https://doi.org/10.5772/29091

Figueiredo MM, Gamelas JA, Martins AG (2012) Characterization of bone and bone-based graft materials using FTIR spectroscopy. In: Theophile T (ed) Infrared spectroscopy-

life and biomedical sciences. https://doi.org/10.5772/36379
Franzel W, Gerlach R (2009) The irradiation action on human dental tissue by X-rays and electrons—a nanoindenter study. Zeitschrift für Medizinische Physik 19(1):5–10. https://doi.org/10.1016/j.zemedi.2008.10.009
Fredericks JD, Bennett P, Williams A, Rogers KD (2012) FTIR spectroscopy: a new diagnostic tool to aid DNA analysis from heated bone. Forensic Sci Int Genet 6(3):375–380. https://doi.org/10.1016/j.fsigen.2011.07.014
Freeman JJ, Wopenka B, Silva MJ, Pasteris JD (2001) Raman spectroscopic detection of changes in bioapatite in mouse femora as a function of age and in vitro fluoride treatment. Calcif Tissue Int 68:156–162. https://doi.org/10.1007/s002230001206
Gamsjaeger S, Robins SP, Tatakis DN, Klaushofer K, Paschalis EP (2017) Identification of pyridinolinetrivalentcollagen cross-links by ramanmicrospectroscopy. Calcif Tissue Int 100:565–574. https://doi.org/10.1007/s00223-016-0232-5
Garnero P (2012) The contribution of collagen crosslinks to bone strength. Bonekey Rep 1:182. https://doi.org/10.1038/bonekey.2012.182
Glimcher MJ (1998) The nature of the mineral phase in bone: biological and clinical applications. In: Alvioli L, Krane S, editors. Metabolic Bone Disease and Clinically Related Disorders, Academic press, p. 23–50. https://doi.org/10.1016/B978-012068700-8/50003-7
Hagiwara K, Goto T, Araki M, Miyazaki M, Hagiwara H (2011) Olive polyphenol hydroxytyrosol prevents bone loss. Eur J Pharmacol 662(1–3):78–84. https://doi.org/10.1016/j.ejphar.2011.04.023
Kairiyama E, Horak C, Spinosa M, Pachado J, Schwint O (2009) Radiation sterilization of skin allograft. Radiat Phys Chem 78(7–8):445–448. https://doi.org/10.1016/j.radphyschem.2009.03.078
Kaminski A, Uhrynowska-Tyszkiewicz I, Stachowicz W (2010) Sterilisation by irradiation. In: Galea G, editor. Essentials of Tissue Banking; p. 123–138. https://doi.org/10.1007/978-90-481-9142-0_9
Kattaya SA, Akkus O, Slama J (2008) Radioprotectant and radiosensitizer effects on sterility of gamma-irradiated bone. Clin Orthop Relat Res 466:1796–1803. https://doi.org/10.1007/s11999-008-0283-7
Krimm S, Bandekar J (1980) Vibrational analysis of peptides, polypeptides, and proteins. V. normal vibrations of beta-turns. Biopolymers 19:1–29. https://doi.org/10.1002/bip.1980.360190102
Kubisz L, Połomska M (2007) FT NIR Raman studies on gamma-irradiated bone. Spectrochim Acta A Mol Biomol Spectrosc 66(3):616–625. https://doi.org/10.1016/j.saa.2006.04.003
Lopes CCA, Limirio PHJO, Novais VR, Dechichi P (2018) Fourier transform infrared spectroscopy (FTIR) application chemical characterization of enamel, dentin and bone. Appl Spectrosc Rev 53(9):1–23. https://doi.org/10.1080/05704928.2018.1431923
Martínez L, Ros G, Nieto G (2018) Hydroxytyrosol: health benefits and use as functional ingredient in meat. Medicines (Basel) 5(1):13. https://doi.org/10.3390/medicines5010013
Mata-Miranda MM, Guerrero-Ruiz M, Gonzalez-Fuentes JR, Hernandez-Toscano CM, Garcia-Andino JR, Sanchez-Brito M, Vazquez-Zapien GJ (2019) Characterization of the biological fingerprint and identification of associated parameters in stress fractures by FTIR spectroscopy. Biomed Res Int. https://doi.org/10.1155/2019/1241452
Mavrogenis AF, Kyriakidou M, Kyriazis S, Anastassopoulou J (2016) Fourier transform infrared spectroscopic studies of radiation-induced molecular changes in bone and cartilage. Expert Rev Qual Life Cancer Care 1(6):459–469. https://doi.org/10.1080/23809000.2016.1254553
McNerny EM, Gong B, Morris MD, Kohn DH (2015) Bone fracture toughness and strength correlate with collagen cross-link maturity in a dose-controlled lathyrism mouse model. J Bone Miner Res 30:455–464. https://doi.org/10.1002/jbmr.2356
Medina-Martínez MS, Truchado P, Castro-Ibáñez I, Allende A (2016) Antimicrobial activity of hydroxytyrosol: a current controversy. Biosci Biotechnol Biochem 80(4):801–810. https://doi.org/10.1080/09168451.2015.1116924
Minamisawa I, Itoman M, Maehara H, Kobayashi A, Watanabe T (1995) Bone banking and sterilization of bones. Radiat Phys Chem 46(2):287–291. https://doi.org/10.1016/0969-806X(95)00026-T
Nagy G, Lorand T, Patonai Z, Montsoko G, Bajnoczky I, Marcsik A, Mark L (2008) Analysis of pathological and non-pathological human skeletal remains by FT-IR spectroscopy. Forensic Sci Int 175(1):55–60. https://doi.org/10.1016/j.forsciint.2007.05.008
Noor Z, Sumitro SB, Hidayat M, Rahim AH, Taufiq A (2011) Assessment of microarchitecture and crystal structure of hydroxyapatite in osteoporosis. Univ Med 30(1):29–35. https://univmed.org/ejurnal/index.php/medicina/article/view/188
Nguyen H, Morgan DA, Forwood MR (2007) Sterilization of allograft bone: effects of gamma irradiation on allograft biology and biomechanics. Cell Tissue Bank 8:93–105. https://doi.org/10.1007/s10561-006-9020-1
Olsen J, Heinemeier J, Bennike P, Krause C, Hornstrup KM, Thrane H (2008) Characterization and blind testing of radiocarbon dating of cremated bone. J Archaeo Sci 35:791–800. https://doi.org/10.1016/j.jas.2007.06.011
Paredes WEB, Geraldo ABC, Andrade DA (2017) ATR-FTIR assessment of the biochemical composition and micro hardness of the hard tissues of oral cavity submitted to gamma irradiation. J Cancer Sci Ther 9(4):379–388. https://doi.org/10.4172/1948-5956.1000446
Paschalis EP, DiCarlo E, Betts F, Sherman P, Mendelsohn R, Boskey AL (1996) FTIR microspectroscopic analysis of human osteonal bone. Calcif Tissue Int 59:480–487. https://doi.org/10.1007/BF00369214
Paschalis EP, Gamsjaeger S, Klaushofer K (2017) Vibrational spectroscopic techniques to assess bone quality. Osteoporos Int 28:2275–2291. https://doi.org/10.1007/s00198-017-4019-y
Pleshko N, Boskey A, Mendelsohn R (1991) Novel infrared spectroscopic method for the determination of crystallinity of hydroxyapatite minerals. Biophys J 60:786–793. https://doi.org/10.1016/S0006-3495(91)82113-0
Potdevin G, Malecki A, Biernath T, Bech M, Jensen TH, Feidenhans'l R, Zanette I, Weitkamp T, Kenntner J, Mohr J,

Roschger P, Kerschnitzki M, Wagermaier W, Klaushofer K, Fratzl P, Pfeiffer F (2012) X-ray vector radiography for bone micro-architecture diagnostics. Phys Med Bio 57:3451–3461. https://doi.org/10.1088/0031-9155/57/11/3451

Puel C, Mardon J, Agalias A, Davicco MJ, Lebecque P, Mazur A, Horcajada MN, Skaltsounis AL, Coxam V (2008) Major phenolic compounds in olive oil modulate bone loss in an ovariectomy/inflammation experimental model. J Agric Food Chem 56(20):9417–9422. https://doi.org/10.1021/jf801794q

Querido W, Ailavajhala R, Padalkar M, Pleshko N (2018) Validated approaches for quantification of bone mineral crystallinity using transmission fourier transform infrared (FT-IR), attenuated total reflection (ATR) FT-IR, and raman spectroscopy. Appl Spectrosc 72(11):1581–1593. https://doi.org/10.1177/0003702818789165

Radzki RP, Bienko M, Wolski D, Lis A, Radzka A (2016) Lipoic acid stimulates bone formation in ovariectomized rats in a dose-dependent manner. Can J Physiol Pharmacol 94(9):947–954. https://doi.org/10.1139/cjpp-2015-0439

Rana MA, Akhtar N, Rahman S, Jamil HM, Asaduzzaman SM (2017) Extraction of hydroxyapatite from bovine and human cortical bone by thermal decomposition and effect of gamma radiation: a comparative study. Int J Complement Altern Medic 8(3):00263. https://doi.org/10.15406/ijcam.2017.08.00263

Rey C, Renugopalakrishnan V, Shimizu M, Collins B, Glimcher MJ (1991) A resolution-enhanced Fourier transform infrared spectroscopic study of the environment of the $CO_3^{(2-)}$ ion in the mineral phase of enamel during its formation and maturation. Calcif Tissue Int 49:259–268. https://doi.org/10.1007/BF02556215

Rietjens SJ, Bast A, Haenen GRMM (2007) New insights into controversies on the antioxidant potential of the olive oil antioxidant hydroxytyrosol. J Agric Food Chem 55(18):7609–7614. https://doi.org/10.1021/jf0706934

Roberts JL, Moreau R (2015) Emerging role of alpha-lipoic acid in the prevention and treatment of bone loss. Nutr Rev 73(2):116–125. https://doi.org/10.1093/nutrit/nuu005

Saito M, Marumo K (2010) Collagen cross-links as a determinant of bone quality: a possible explanation for bone fragility in aging, osteoporosis, and diabetes mellitus. Osteoporos Int 21:195–214. https://doi.org/10.1007/s00198-009-1066-z

Sasso GD, Asscher Y, Angelini I, Nodari L, Artioli G (2018) A universal curve of apatite crystallinity for the assessment of bone integrity and preservation. Sci Rep 8:12025. https://doi.org/10.1038/s41598-018-30642-z

Seema A, Kattaya MS, Akkus O (2008) Radioprotectant and Radiosensitizer Effects on Sterility of gamma-irradiated Bone. Clin Orthop Relat Res 466:1796. https://doi.org/10.1007/s11999-008-0283-7

Self WT, Tsai L, Stadman TC (2000) Synthesis and characterization of selenotrisulfide derivatives of lipoic acid and lipoamide. Proc Natl Acad Sci 97(23):12481–12486. https://doi.org/10.1073/pnas.220426897

Seto A, Gatt CJ Jr, Dunn MG (2009) Improved tendon radioprotection by combined cross-linking and free radical scavenging. Clin Orthop Relat Res 467:2994–3001. https://doi.org/10.1007/s11999-009-0934-3

Severcan F, Haris PI (2012) Introduction to vibrational spectroscopy in diagnosis and screening. In: Severcan F, Haris PI (ed) Advances in biomedical spectroscopy, vo 6; p. 1–11. https://doi.org/10.3233/978-1-61499-059-8-1

Singh R, Singh D, Singh A (2016) Radiation sterilization of tissue allografts: a review. World J Radiol 8(4):355–369. https://doi.org/10.4329/wjr.v8.i4.355

Smith AR, Shenvi SV, Widlansky M, Suh JH, Hagen TM (2004) Lipoic acid as a potential therapy for chronic disease associated with oxidative stress. Curr Med Chem 11(9):1135–1146. https://doi.org/10.2174/0929867043365387

Sun H, Fu C, Wang CY, Jin Y, Liu O, Meng Q, Liu KX (2014) Alpha-lipoic acid produces bone-protective effects via modulating Nox4/ROS/NF-κB and Wnt/ Lrp5/β-catenin signaling pathways in H2O2-treated MC3T3-E1 cells and ovariectomy rats. 3rd International Summit on Toxicology & Applied Pharmacology DoubleTree by Hilton Hotel Chicago-North Shore, USA 4:4. https://doi.org/10.4172/2161-0495.S1.012

Surovell TA, Stiner MC (2001) Standardizing Infra-red measures of bone mineral crystallinity: an experimental approach. J Archaeol Sci 28(6):633–642. https://doi.org/10.1006/jasc.2000.0633

Tami AE, Schaffler MB, Knothe Tate ML (2003) Probing the tissue to subcellular level structure underlying bone's molecular sieving function. Biorheology 40(6):577–590. PMID: 14610309

Unal M, Creecy A, Nyman JS (2018) the role of matrix composition in the mechanical behavior of bone. Curr Osteoporos Rep 16:205–215. https://doi.org/10.1007/s11914-018-0433-0

Veloso MN, Santin SP, Benetti C, Pereira TM, Mattor MB, Politano R, Zezell DM (2013) Evaluation of ionizing radiation effects in bone tissue by FTIR Spectroscopy and Dynamic Mechanical analysis. International Nuclear Atlantic Conference (INAC), Brazil. https://inis.iaea.org/search/search.aspx?orig_q=RN:46012958

Vidal Bde C, Mello ML (2011) Collagen type I amide I band infrared spectroscopy. Micron 42(3):283–289. https://doi.org/10.1016/j.micron.2010.09.010

Vilaplana-Pérez C, Auñón D, García-Flores LA, Gil-Izquierdo A (2014) Hydroxytyrosol and potential uses in cardiovascular diseases, cancer, and AIDS. Front Nutr 1(18):1–11. https://doi.org/10.3389/fnut.2014.00018

Wang XY, Zuo Y, Huang D, Hou XD, Li YB (2010) Comparative study on inorganic composition and crystallographic properties of cortical and cancellous bone. Biomed Environ Sci 23(6):473–480. https://doi.org/10.1016/S0895-3988(11)60010-X

Wang X, Shen X, Li X, Agrawal CM (2002) Age-related changes in the collagen network and the toughness of bone. Bone 31(1):1–7. https://doi.org/10.1016/S8756-3282(01)00697-4

Wang X, Bank RA, TeKoppele JM, Agrawal CM (2001) The role of collagen in determining bone mechanical properties. J Orthop Res 19:1021–1026. https://doi.org/10.1016/S0736-0266(01)00047-X

Weiner S, Bar-Yosef O (1990) States of preservation of bones from prehistoric sites in the Near East: a survey. J Archaeo

Sci 17(2):187–196. https://doi.org/10.1016/0305-4403(90)90058-D

Wen XX, Wang FQ, Xu C, Wu ZX, Zhang Y, Feng YF, Yan YB, Lei W (2015) Time related changes of mineral and collagen and their roles in cortical bone mechanics of ovariectomized rabbits. PLoS ONE 10(6):e0127973. https://doi.org/10.1371/journal.pone.0127973

Willett TL, Burton B, Woodside M, Wang Z, Gaspar A, Attia T (2015) γ-Irradiation sterilized bone strengthened and toughened by ribose pre-treatment. J Mech Behav Biomed Mater 44:147–155. https://doi.org/10.1016/j.jmbbm.2015.01.003

Yerramshetty JS, Akkus O (2008) The associations between mineral crystallinity and the mechanical properties of human cortical bone. Bone 42(3):476–482. https://doi.org/10.1016/j.bone.2007.12.001

Yerramshetty JS, Lind C, Akkus O (2006) The compositional and physicochemical homogeneity of male femoral cortex increases after the sixth decade. Bone 39(6):1236–1243. https://doi.org/10.1016/j.bone.2006.06.002

Zezell DM, Benetti C, Veloso MN, Castro PAA, Ana PA (2015) FTIR spectroscopy revealing the effects of laser and ionizing radiation on biological hard tissues. J Braz Chem Soc 26(12):2571–2582. https://doi.org/10.5935/0103-5053.20150246

Zioupos P, Currey JD, Hamer AJ (1999) The role of collagen in the declining mechanical properties of aging human cortical bone. J Biomed Mater Res 45(2):108–116. https://doi.org/10.1002/(SICI)1097-4636(199905)45:2%3c108::AID-JBM5%3e3.0.CO;2-A